Journal of Hazardous Materials 185 (2011) 1073–1080

Contents lists available at ScienceDirect

Journal of Hazardous Materials

journal homepage: www.elsevier.com/locate/jhazmat

Removal of fluoride from aqueous solution using granular acid-treated bentonite (GHB): Batch and column studies

Yuxin Ma[a,b,*], Fengmei Shi[c], Xilai Zheng[d], Jun Ma[c], Congjie Gao[a]

[a] College of Chemistry and Chemical Engineering, Ocean University of China, Qingdao 266100, China
[b] College of Architecture and Civil Engineering, Heilongjiang University, Harbin 150080, China
[c] State Key Laboratory of Urban Water Resource and Environment, Harbin Institute of Technology, Harbin 150090, China
[d] College of Environmental Science and Engineering, Ocean University of China, Qingdao 266100, China

ARTICLE INFO

Article history:
Received 21 April 2010
Received in revised form 20 July 2010
Accepted 5 October 2010
Available online 1 November 2010

Keywords:
Granular acid-treated bentonite (GHB)
Fluoride removal
Adsorption
Dubinin–Rasdushkevich (D–R) equation
Thomas model
Regeneration

ABSTRACT

Removal of fluoride from aqueous solution using granular acid-treated bentonite (GHB) was studied by batch and column adsorption experiments. The results of the batch adsorption experiments demonstrated that the maximum fluoride removal was obtained at pH of 4.95 and it took 40 min to attain equilibrium. Kinetics data fitted pseudo-second-order model. Batch adsorption data was better described by Redlich–Peterson and Freundlich isotherm models than Langmuir isotherm model. The adsorption type of GHB was ion exchange. Column experiments were carried out at different influent fluoride concentrations and different flow rates. The capacities of the breakthrough and exhaustion points increased with the decrease of flow rate and the increase of initial fluoride concentration. The experimental results were well fitted with Thomas model. Exhausted GHB was regenerated by alkali/alum treatment. The total sorption capacity of GHB was increased after regeneration and activation.

1. Introduction

Endemic fluorosis caused by fluoride in excess is a global geochemical disease [1]. Maintaining fluoride concentration of 1 mg/L in the dietary intake can prevent skeletal and dental problems. However, when the fluoride concentration is above this level, it leads to dental and skeletal fluorosis and lesions of the endocrine glands, thyroid and liver. According to the World Health Organization (WHO), the maximum acceptable concentration of fluoride is 1.5 mg/L [2]. It is therefore necessary to remove the excessive fluoride from drinking water if the fluoride concentration is higher than 1.5 mg/L.

Many methods, i.e. adsorption [3,4], ion exchange [5], precipitation [6], Donnan dialysis [7–10], electrodialysis [11], reverse osmosis [12], nanofiltration [13] and ultrafiltration [14] have been investigated to remove excessive fluoride from water. Among these methods, adsorption is still one of the most extensively used methods. Recent attention of scientists has been devoted to the study of different types of low cost materials such as kaolinite, bentonite, charfine, lignites, sirmali seeds [15], waste mud [16], calcite [17], amorphous alumina [18], bleaching earth [19], red mud [3], gas concrete material [20], montmorillonite [4], etc., for adsorption of fluoride from water.

Bentonite is a sediment (usually) composed of smectite [21]. The bentonites are widespread in most continents of the world and its low cost makes it a strong candidate as an adsorbent for the removal of many pollutants from wastewaters. Studies have shown its ability to bind and remove pathogenic viruses, pesticides, herbicides, rare earth elements, heavy metals and other toxins [19]. Bentonite can sorb fluoride in the acid conditions and has pH dependency [4,22,23].

Although it can adsorb many pollutants, its use as an adsorbent in a filtration mode is limited in practice for the following reasons: (i) bentonite on contact with water swells and forms a highly stable colloidal suspension, making its separation from water following adsorption very difficult; and (ii) the use of bentonite as an adsorbent material in columns is limited by the low permeability of the compacted bentonite bed [24].

Kapoor and Viraraghavan [24] immobilized bentonite with polysulfone and made beads with surface area of up to 20 m^2/g. The beads were able to remove more than 99% of copper and cadmium ions in the column mode. Zhu et al. [25] and Tor et al. [26] prepared granular red mud (GRM) as low-cost adsorbent to remove cadmium ions and fluoride ion from water, respectively. The method

* Corresponding author at: College of Architecture and Civil Engineering, Heilongjiang University, Harbin 150080, China. Tel.: +86 451 86604021; fax: +86 451 86604021.
E-mail address: oucmyx@126.com (Y. Ma).

0304-3894/$ – see front matter © 2010 Elsevier B.V. All rights reserved.
doi:10.1016/j.jhazmat.2010.10.016

Nomenclature

b	Langmuir isotherm constant (L/mg)
C	the effluent fluoride concentration (mg/L) (g/L for DR equation)
C_0	the initial fluoride concentration or the influent fluoride concentration (column) (mg/L)
C_B	the effluent fluoride concentration at the breakthrough point (mg/L)
C_E	the effluent fluoride concentration at the exhaustion point (mg/L)
C_e	the fluoride concentration at equilibrium or the effluent fluoride concentration (column) (mg/L)
E	the mean free energy of adsorption (kJ/mol)
f	a parameter measuring the symmetry of the breakthrough curve
F_0	flow rate of fluoride solution (mL/min)
H	the bed depth (cm)
h_Z	the height of the mass transfer zone (cm)
K	the constant of DR equation related to the adsorption energy
k_F, n	Freundlich isotherm constant
K_R, a_R, β	Redlich–Peterson isotherm constant
k_T	the rate constant of Thomas model (L mg^{-1} h^{-1})
k_1	the adsorption rate constant of first-order adsorption (L/min)
k_2	the rate constant of pseudo-second-order chemisorption (g/(mg min))
m	the adsorbent dosage or the mass of the sorbent (g)
q_B	the capacity at the breakthrough point (mg/g)
q_E	the capacity at the exhaustion point (mg/g)
q_e	the amounts of fluoride adsorbed at equilibrium (mg/g)
q_t	the amounts of fluoride adsorbed at time t (min) (mg/g)
q_T	the total sorption capacity (mg/g)
Q	the fluoride adsorbed (mg/g)
Q^0	Langmuir constant related to the capacity and energy of adsorption (mg/g)
R	the gas constant (kJ/(K mol))
T	the temperature (K)
V	the solution volume or the effluent volume (column) (L)
V_B	the volume of solution passed up to the breakthrough point (L)
V_E	the volume of solution passed up to the exhaustion point (L)
X	the amount of fluoride adsorbed per unit weight of adsorbent (g/g)
X_m	the adsorption capacity per unit weight of adsorbent (g/g)

Greek symbols

θ	the flow rate (L/h)
ε	polanyi potentiali = $RT\ln(1+(1/C))$

to prepare beads is easier to realize, but the introduction of polysulfone may increase the hydrophobicity of the prepared beads. It is necessary to prepare GHB with PVA which is hydrophilic in nature.

The objective of the study was to: (i) develop a procedure for fabrication of GHB with PVA, (ii) examine fluoride adsorption capacity of GHB by batch studies, (iii) investigate the fluoride uptake characteristics of GHB by column studies.

2. Materials and methods

2.1. Bentonite used

The bentonite used was a natural Ca–bentonite. Its grain size was less than 200 mesh. Its chemical composition by structural formula was: $(K_{0.036}Na_{0.121}Ca_{0.336}Mg_{0.004})(Al_{2.893}Fe^{3+}{}_{0.288}Fe^{2+}{}_{0.003})[Si_{7.921}Al_{0.079}]O_{21}(OH)_4$ [27].

2.2. Preparation of GHB

H-bentonite preparation: 30 g Ca–bentonite which was calcinated at 300 °C for 2 h was dispersed into 100 mL distilled water in a 200 mL flask mounted in a water bath at a temperature of 95 ± 2 °C. 10 mL of 1 M HCl solution was added and stirred for 6 h. The solution was centrifuged and washed with distilled water for 3–5 times until no Cl^- was detected with $AgNO_3$ solution as an indicator. The bentonite was dried at 105 °C for 4 h. The dried sample was grinded and passed through the 200 mesh sieve.

GHB was prepared by dried H–bentonite and analytical grade PVA. 20 g PVA and 250 mL distilled water were put into a 500 mL beaker in water bath at 95–98 °C until PVA ultimately dissolved. 130 g H–bentonite was added to the PVA solution. The sample was stirred by mechanical stirrer and then dried in vacuo at 60 °C. The dried sample was grinded and sieved. In order to improve the stability, GHB was cross-linked in 0.5% glutaraldehyde solution (50 °C, pH = 3–4) for 30 min. GHB with 0.15–0.42 mm was used in the study.

The N_2-adsorption and desorption, at liquid N_2 temperature on and from the H–bentonite and GHB samples were determined by a volumetric Pyrex glass adsorption instrument connected to high vacuum.

2.3. Batch adsorption experiments

The fluoride solutions were prepared by diluting the prepared stock solution (1000 mg/L NaF, prepared in laboratory) to desired concentrations. All experiments were carried out at a constant ionic strength of 0.01 M maintained with NaCl. 6.00 g of GHB and fluoride solution were taken in a 500 mL stoppered conical flask. 20 mL of 0.1 M sodium chloride was added to maintain ionic strength, and pH was adjusted to the desired level with 0.1 M NaOH or 0.1 M HCl solutions. The final volume of the solution was 200 mL. The solution was shaken at constant speed (400 rpm) with shaker at 25 ± 1 °C over a period of time and filtrated with a 0.45 μm cellulose acetate membrane without centrifugation. Final pH and F^- levels were measured by the appropriate electrodes.

All ion selective and pH electrodes used were connected to an Orion 720A pH/ISE meter. Fluoride measurements were performed with the Orion 94-09 fluoride and reference electrodes. The detection limit of the electrodes is 0.02 mg/L, measurement reproducibility is 2% and there are no interference effects from anions commonly associated with F^-. Complexed F measurements were made on aliquots of filtrate prediluted with an equal amount of TISAB (total ion strength adjustment buffering). Each litre of TISAB contained 1 mol of NaCl, 1 mol of CH_3COOH, 4 g of CDTA (1,2-cyclohexylenedinitrilotetraacetic acid) and sufficient NaOH to yield a final pH of 5.0–5.5. The CDTA in TISAB was the decomplexing agent that released all complexed F into free F ions, which were then measurable with the ISE. pH measurements in the solution were performed with an Orion 81-02 pH electrode. The detection limit is noted at 0.01 pH. The amount of fluoride adsorbed was calculated from the following equation:

$$q = \frac{(C_0 - C_e)V}{m} \quad (1)$$

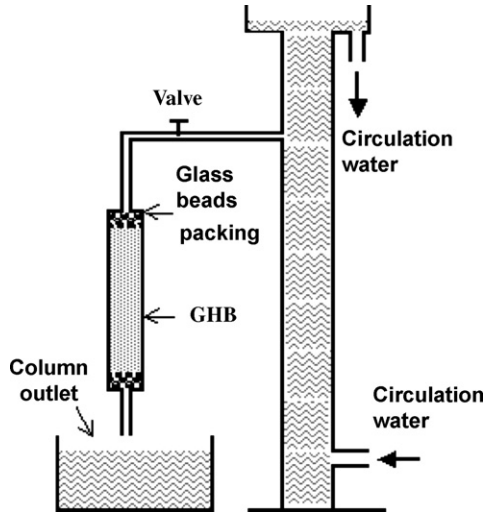

Fig. 1. Schematic diagram of experimental setup for column study.

where q is the fluoride adsorbed (mg/g), C_0 is the initial concentration of fluoride (mg/L), C_e is the concentration of fluoride in solution at equilibrium time (mg/L), V is the solution volume (L), and m is the mass of the sorbent (g). The experimental parameters studied are contact time (5–120 min), initial fluoride concentration (2.85–20 mg/L), and pH (2.65–11.65).

2.4. Column adsorption experiments

Column studies were conducted at room temperature in a glass column (1.767 cm^2 of cross-sectional area and 40 cm of height). 57.60 g GHB was packed in the glass column and it resulted in a bed height of 28.0 cm and used as fixed bed down-flow reactors. For column experiments, a column (i.d. 100 mm, length 420 mm) was used with a feed reservoir of 20 L capacity at the top of the column. The inlet flow rate was controlled by a flow controller. The synthetic sample solution was circulated with a pump and a reservoir in order to attain the constant water level. For the uniform distribution of liquid, glass beads were placed above the adsorbent. The schematic experimental setup for the column experiments was shown in Fig. 1. The columns were operated using downward flow at $25 \pm 1\,^{\circ}C$ in the air conditioned laboratory.

Flow rates of 2.42 and 8.35 mL/min were used to study the effect of the flow rate on fluoride removal. The columns were run using water containing 2.85 mg/L or 6.34 mg/L of fluoride with a pH of 7.10. Flow rates were checked by physically collecting the discharge from column for a given time and measuring the volume collected. After exhaustion of the column, desorption studies were carried out using 0.1 M NaOH and reactivated by immersing GHB in the 1% $KAl(SO_4)_2$ solution for 12 h. The capacity at the breakthrough point (q_B) is defined as the amount of fluoride ions bound by GHB when the concentration of fluoride in the effluent reaches ≈5% of the initial concentration [28].

$$q_B = \int_0^{C_B} \frac{(C_0 - C)dV}{m} \tag{2}$$

where q_B is the capacity at the breakthrough point (mg/g), C_0 is the influent fluoride concentration (mg/L), C is the effluent fluoride concentration (mg/L), m is the mass of the sorbent (g), and V_B is the volume of solution passed up to the breakthrough point (L). The capacity at the exhaustion point (q_E) corresponds to the amount of fluoride ions bound by GHB when the concentration of fluoride in the effluent reaches ≈95% of the initial value [28].

$$q_E = \int_0^{C_E} \frac{(C_0 - C)dV}{m} \tag{3}$$

where q_E is the capacity at the exhaustion point (mg/g), V_E is the volume of solution passed up to the exhaustion point (L), and C_0, C and m are defined as the same as above.

2.5. Column regeneration studies

To retrieve the GHB sorbents and reuse saturated column, regeneration experiments were conducted using alkali/alum treatment. In present study, the column previously run under "8.35 mL/min of flow rate" was chosen in desorption experiments on account of representativeness.

Regenerants used to regenerate or reactivate exhausted GHB included NaOH and $KAl(SO_4)_2$. Exhausted GHB was dipped in 50 mL 0.1 M NaOH for 12 h and washed repeatedly for 2–3 times with 50 mL distilled water each time, then transferred to a flask containing 30 mL 1% $KAl(SO_4)_2$ solution undergoing activation for 12 h. Subsequent distilled water washing was carried to raise the pH to 7 followed by drying in oven at 105 °C for 2 h. The reactivated GHB was ready for the next defluoridation cycle.

3. Results and discussion

The voids in a solid structure with widths smaller than 2 nm, between 2 nm and 50 nm, and greater than 50 nm are called micropores, mesopores, and macropores respectively. Pore-volume, surface area and pore size range of H-bentonite and GHB were shown in Table 1. The specific surface area of the H–bentonite and GHB are 213.0 m^2/g and 24.5 m^2/g, respectively. GHB has a majority of micropores and macropores, which is different from the H-bentonite. Part of PVA was intercalated into the layers of bentonite and increased the layer space, also decreased the micropores volume. The binding of PVA with H–bentonite brought about macropores in the GHB. The micropores acts as adsorption sites and macropores acts as channels. It is a kind of heterogeneous adsorption.

3.1. Batch adsorption experiments

3.1.1. Effect of contact time and adsorption kinetics

The equilibrium time for the F^- adsorption reaction was defined as the agitation period necessary for the F^- concentration in solution to achieve a steady state. The removal of fluoride as a function of contact time was shown in Fig. 2. It was observed that with a fixed amount of GHB, the removal of fluoride increased with time and then attained equilibrium after 40 min. Thus, all subsequent samples employed 1 h reaction time.

The experimental adsorption data was analyzed by application of the pseudo-first-order and pseudo-second-order kinetic models. The linearized form of pseudo-first-order rate equation is given as [29]

$$\log(q_e - q_t) = \log q_e - \frac{k_1 t}{2.303} \tag{4}$$

where q_e and q_t are the amounts of fluoride adsorbed (mg/g) at equilibrium and at time t (min), respectively, and k_1 (L/min) is the adsorption rate constant of first-order adsorption.

For the studied initial concentrations, the rate constant (k_1) and theoretical equilibrium sorption capacities, q_e (calculated), calculated from the slope and intercept of the linear plots of the pseudo-first-order kinetic model, and the coefficient of determination (R^2) were given in Table 2. In addition, theoretical and experimental q_e values were in a good accordance with each other.

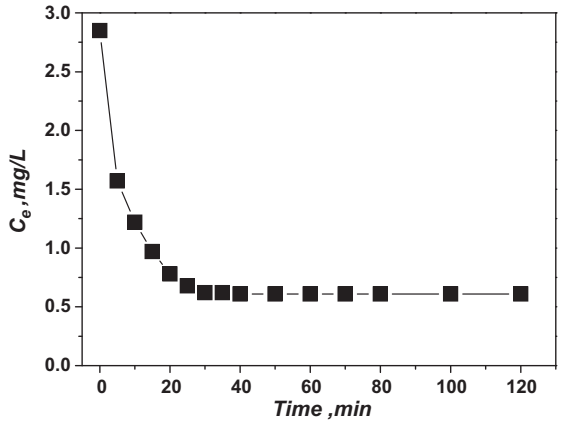

Fig. 2. Effect of reaction time on the fluoride concentration of the solutions. Experimental conditions: C_0 = 2.85 mg/L; temperature, 25 ± 1 °C; shaken speed, 400 rpm; GHB dosage, 30 g/L; pH_i = 7.11.

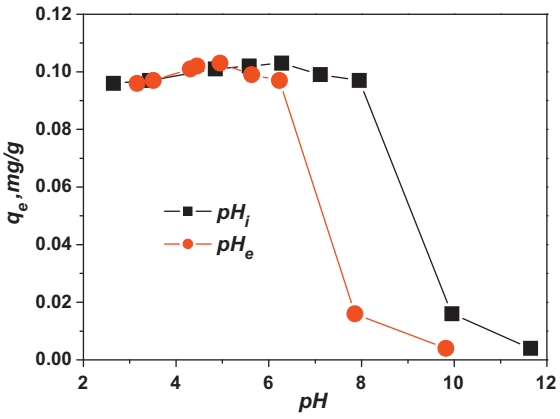

Fig. 3. Effect of pH values in the solutions on the fluoride adsorbed. Experimental conditions: C_0 = 5.0 mg/L; temperature, 25 ± 1 °C; shaken speed, 400 rpm; GHB dosage, 30 g/L; pH_i = 2.65, 3.43, 4.85, 5.58, 6.28, 7.11, 7.95, 9.95, 11.65.

Therefore, it could be suggested that the adsorption of fluoride by GHB followed the first-order type reaction kinetics.

The experimental data was also applied to the pseudo-second-order kinetic model given as

$$\frac{dq_t}{dt} = k_2(q_e - q_t)^2 \quad (5)$$

where k_2 is the rate constant of pseudo-second-order chemisorption (g/(mg min)). For boundary conditions (t = 0 to $t = t$ and q_t = 0 to $q_t = q_t$), pseudo-second-order kinetic model of Ho and McKay [30,31] is:

$$\frac{t}{q_t} = \frac{1}{k_2 q_e{}^2} + \frac{t}{q_e} \quad (6)$$

The constants calculated from the slope and intercept of the plots were given in Table 2. It can be seen from the results in Table 2 that q_e (calculated) and q_e (experimental) values were in agreement with each other. The coefficient of determination of second-order type reaction (R^2 = 0.9986) is larger than that of first-order type reaction (R^2 = 0.9820). Therefore, it was possible to suggest that the sorption of fluoride by GHB was a second-order type reaction.

3.1.2. Effect of pH

The effect of pH on the sorption of fluoride was shown in Fig. 3. At lower initial pH value (pH_i), the amount of F^- adsorbed at equilibrium (q_e) increased slightly with the increase of pH_i in the solution. When pH_i increased from 2.65 to 6.28, the equilibrium pH value (pH_e) changed from 3.16 to 4.95, q_e increased from 0.096 mg/g to 0.103 mg/g and attained the maximum. When pH_i was higher than 6.28, q_e decreased with the increase of pH_i and had a value of 0.004 mg/g at pH_i of 11.65 (pH_e = 9.83). When pH_i was between 2.65 and 7.95 (pH_e = 3.16–6.23), q_e value was more than 0.095 mg/g. The range was the optimum pH for GHB defluoridation. This may be explained by considering the zero point of charge (pH_{zpc}) for the GHB. Zero point of charge is a concept in physical chemistry relating to the phenomenon of adsorption, and it describes the condition when the electrical charge density on a surface is zero. In other words, is (usually) the pH value at which a solid submerged in an electrolyte exhibits zero net electrical charge on the surface. Although pH_{zpc} is still uncertain, there are several colloid chemical arguments that it must be near pH ~ 5 for montmorillonite [32,33]. The metal oxides in GHB formed aqua complexes with water and developed a charged surface through amphoteric dissociation. From the results, we can conclude the pH_{zpc} of GHB is near to 4.95. If the pH was above pH_{zpc}, more of the surface sites were negatively charged and F^- will be adsorbed to a lesser extent due to the repulsive forces between F^- ions and negative charge of the GHB surface [26]. If the pH was below pH_{zpc}, the surface charge is positive, more fluoride ion should be adsorbed, but the results show the opposite. In lower pH value, more F^- ions react with H^+ ions and form HF molecules which are neutral and difficult to be adsorbed by GHB.

It is known that clay minerals possess attractive properties as solid acids [34,35]. Their acidities are due to active centers on the surface that exhibit Bronsted and Lewis acidities and govern most of

Table 1
Pore-volume, surface area and pore size range of H-bentonite and GHB.

Sample	Specific surface area (m^2/g)	Pore type	Specific pore volume (cm^3/g)	Pore size range (nm)
H–bentonite	213.0	Micropore	0.0572	0.7–2.0 (mainly 1.5–1.7)
		Mesopore	0.1213	2–20 (mainly 3–5)
		Macropore	0	Not detected
GHB	24.5	Micropore	0.0284	0.8–2.0 (mainly 1.5–1.9)
		Mesopore	0.0897	2–50 (mainly 3–5)
		Macropore	0.1754	50–1000 (mainly 200–500)

Table 2
Values of adsorption rate constant for pseudo-first-order and pseudo-second-order kinetic models (data from Fig. 1).

Experimental result		Pseudo-first-order kinetic model		Pseudo-second-order kinetic model	
q(exp) (mg/g)	0.0747	q(cal) (mg/g)	0.0882 (0.0734–0.1052)[a]	q(cal) (mg/g)	0.0870 (0.0855–0.0885)[a]
		k_1 (1/min)	0.153 ± 0.009[a]	k_2 (g/(mg min))	2.09 (1.89–2.32)[a]
		R^2	0.9820	R^2	0.9986

[a] The range of value is calculated by the standard error.

the clay's interactions in so many application areas. Acid-activated clays exhibit significantly different physicochemical characteristics compared to their non-activated counterparts and one of these physicochemical properties is surface acidity which is a combination of its Bronsted and Lewis acidities [36]. As seen in Fig. 3, the addition of GHB can change the pH value in the solution. At higher pH conditions, pH values decreased owing to the surface acidities of GHB. At lower pH conditions, pH values in the solutions increased by ion exchange of F^- in the solution and OH group on the GHB.

At higher pH conditions, GHB has little sorption of fluoride. Therefore, alkali can be used as a regenerant to adjust the pH in the solution to realize the fluoride desorption and regeneration of exhausted GHB.

3.1.3. Adsorption isotherm models

The analysis of the sorption isotherms was important for design purposes. Therefore, experimental data was analysed with well known sorption isotherm models including the Langmuir (7), Freundlich (8) and Redlich–Peterson isotherms (9) [37–39]

$$\frac{1}{q_e} = \frac{1}{Q^0} + \frac{1}{bQ^0}\frac{1}{C_e} \tag{7}$$

$$\ln q_e = \ln k_F + \frac{1}{n}\ln C_e \tag{8}$$

$$\ln\left[\left(\frac{K_R C_e}{q_e} - 1\right)\right] = \ln a_R + \beta \ln C_e \tag{9}$$

where k_F (mg/g)(L/mg)$^{1/n}$ and $1/n$ are Freundlich constants related to adsorption capacity and adsorption intensity, respectively, of the sorbent. q_e is the amount adsorbed at equilibrium (mg/g), C_e is the equilibrium concentration of the adsorbate (mg/L), and Q^0 (mg/g) and b (L/mg) are the Langmuir constants related to the maximum adsorption capacity and the energy of adsorption, respectively. K_R is the Redlich–Peterson isotherm constant (L/mg), a_R is also a constant (L/mg)$^{\beta}$ and β is the exponent which lies between 0 and 1. For $\beta = 1$, Eq. (8) reduces to Langmuir equation and for $\beta = 0$, it reduces to Henry's equation.

The Langmuir, Freundlich and Redlich–Peterson isotherms and the experimental data were shown in Fig. 4. The isotherm constants and R^2 values for each model were given in Table 3. On the comparison of the R^2 values, it can be concluded that adsorption data can be better described by Redlich–Peterson and Freundlich isotherm models. It was shown from Fig. 2 that Redlich–Peterson model was almost consistent with the Freundlich isotherm model. The result was same to the study of Tor et al. on fluoride removal by using granular red mud (GRM) [26]. It may be attributed to various active sites or heterogeneous mixture of several minerals in GHB which made GHB having different affinities to fluoride ion [26,40]. The comparison of the Freundlich capacity constants of different adsorbents for fluoride adsorption was given in Table 4. The adsorption capacity of GHB is lower than that of adsorbents in the reference because PVA occupied part of mass and the specific surface area was lowered in granular state.

3.1.4. Dubinin–Rasdushkevich (DR) isotherm

It is known that the Langmuir, Freundlich and Redlich–Peterson isotherm constants do not give any idea about the adsorption mechanism. In order to understand the adsorption type, equilibrium data was tested with DR isotherm. DR equation can be written as [41,42]

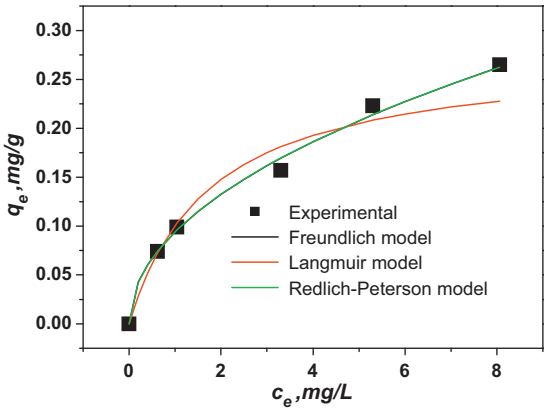

Fig. 4. Fitting of experimental data (points) to curves obtained from the Langmuir, Freundlich and Redlich–Peterson isotherms for fluoride adsorption on GHB. Experimental conditions: temperature, 25 ± 1 °C; shaken speed, 400 rpm; GHB dosage, 30 g/L; pH_i = 7.11; C_0 = 0, 2.85, 5, 10, 15, 20 mg/L.

Table 4
The comparison of the Freundlich capacity constants of different adsorbents for fluoride adsorption.

Adsorbent	k (mg/g)	n	Reference
Neutralized red mud (powdered)	1.14	1.29	[3]
Acid activated red mud (powdered)	5.06	1.97	[3]
Montmorillonite	0.26	1.77	[4]
Spent bleaching earth	0.94	0.46	[19]
Waste mud	1.04–10.79	1.79–2.29	[16]
Amorphous alumina	1.21–9.68	1.36–3.96	[18]
Granular red mud	0.851	2.082	[27]
Granular acid-treated bentonite	0.094	2.082	Present study

$$\ln X = \ln X_m - K\varepsilon^2 \tag{10}$$

where ε (polanyi potentiali) = $RT\ln(1 + (1/C))$, X is the amount of fluoride adsorbed per unit weight of adsorbent (g/g), X_m is the adsorption capacity (g/g), C is the equilibrium concentration of fluoride in aqueous solution (g/L), K is the constant related to the adsorption energy, R is the gas constant [kJ/(K mol)] and T is the temperature (K).

Fig. 5 showed the plot of $\ln X$ against ε^2 with correlation coefficients R^2 = 0.9871. DR isotherm constants, K and X_m were calculated from the slope and intercept of the plot which is -0.0065 ± 0.0004 and 0.6465 ± 0.0667 mg/g respectively.

The mean free energy of adsorption (E), defined as the free energy change when 1 mol of ion is transferred to the surface of the solid from infinity in solution can be calculated from the K-value using the equation:

$$E = (-2K)^{-0.5} \tag{11}$$

The magnitude of the mean free energy of adsorption (E) calculated from DR equation is useful for estimating the type of

Table 3
Langmuir, Freundlich and Redlich–Peterson isotherm parameters for the adsorption of fluoride by GHB (data from Fig. 4).

Langmuir isotherm		Freundlich isotherm		Redlich–Peterson isotherm	
Q^0 (mg/g)	0.278 (0.246–0.319) [a]	K_F (mg/g)(L/g)$^{1/n}$	0.094 ± 0.003[a]	K_R (L/mg)	5.265
b (L/mg)	0.569 (0.524–0.622) [a]	n	2.082 (1.935–2.139)[a]	a_R (L/mg)$^{\beta}$	54.89 (53.10–56.74)[a]
R^2	0.987	R^2	0.993	R^2	0.993

[a] The range of value is calculated by the standard error.

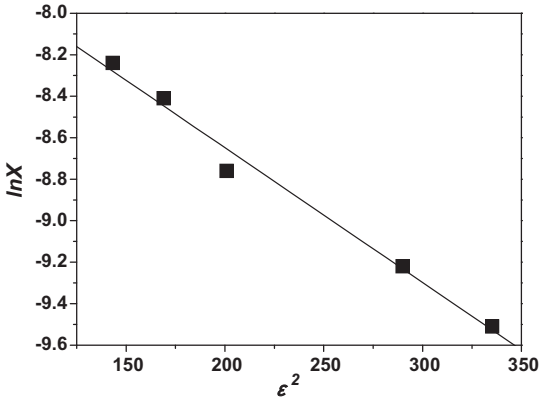

Fig. 5. Dubinin–Rasdushkevich (D–R) plot for the adsorption of fluoride (data from Fig. 4).

adsorption. E value of GHB was 8.77 ± 0.28 kJ/mol (between 8 and 16 kJ/mol), the adsorption type can be explained by ion exchange [42]. F ions in the solution were exchanged with the OH group on the GHB.

3.2. Column adsorption experiments

The breakthrough curve for a column was determined by plotting the ratio of the C_e/C_0 (C_e and C_0 are the fluoride concentration of effluent and influent, respectively) against the time. The breakthrough curves of GHB and regenerated GHB (RGHB) at different flow rate (F_0) and influent fluoride concentration (C_0) were presented in Fig. 6.

During the process, the influent containing fluoride ions passed through the fixed bed of GHB, and a mass transfer zone formed [43]. This zone also moved through the column and reached exit at the exhaustion point. The height of the mass transfer zone (h_Z) can be calculated by the following equation [29]:

$$h_Z = \frac{H(V_E - V_B)}{V_E - (1-f)(V_E - V_B)} \tag{12}$$

where H is the bed depth (cm), f is a parameter which measures the symmetry of the breakthrough curve, or the fraction of GHB present in the bed which is still capable of removing fluoride.

The f can be defined as

$$f = \int_0^1 \left(1 - \frac{C}{C_0}\right) d\left[\frac{V - V_B}{V_E - V_B}\right] = \int_{V_B}^{V_E} \frac{(C_0 - C)dV}{C_0(V_E - V_B)} \tag{13}$$

where V is the effluent volume (L) and the others are defined as the same as above.

The empty bed contact time (EBCT) or the residence time is usually defined as the relation between the depth of the GHB bed in the column and the influent velocity:

$$EBCT = \frac{H}{F_0} \tag{14}$$

where F_0 is the linear flow rate through the column (cm^3/cm^2 min). The parameters in Eqs. (2), (3) and (12)–(14) were calculated from the experimental data and given in Table 5.

It is too difficult to describe the dynamic behavior of compound in a fixed bed under defined operating conditions because the process does not occur at a steady state while the influent still passes through the bed. Various simple mathematical models have been developed to describe and possibly predict the dynamic behavior of the bed in column performance [44]. One of these models used for the continuous flow conditions is the Thomas model [45], which can be written as

$$\frac{C_e}{C_0} = \frac{1}{1 + \exp[k_T(q_T m - C_0 V)/\theta]} \tag{15}$$

where C_e is the effluent fluoride concentration (mg/L), C_0 is influent fluoride concentration (mg/L), k_T is the rate constant (L mg^{-1} h^{-1}), θ is the flow rate (L/h), q_T is the total sorption capacity (mg/g), V is the throughput volume (L), and m is the mass of adsorbent (g).

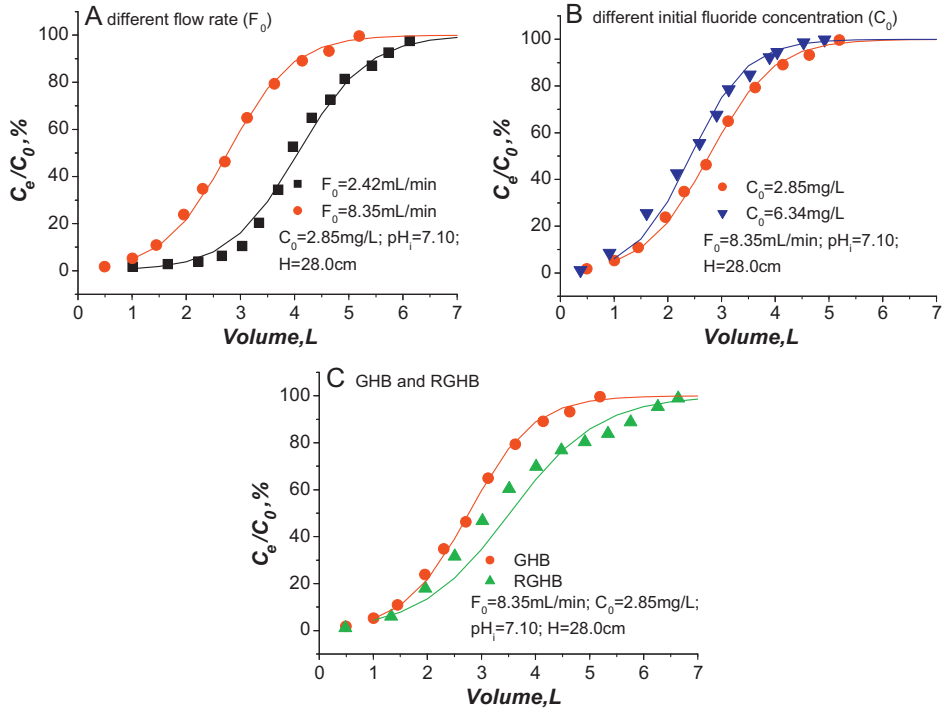

Fig. 6. Breakthrough curves expressed as C_e/C_0 versus time. Fitting of experimental data (points) to curves obtained from the Thomas model (lines).

Table 5
Parameters calculated from the column experimental data (data from Fig. 7).

F_0 (mL/min)	C_0 (mg/L)	q_B (mg/g)	q_E (mg/g)	f	h_Z (cm)	EBCT (min)	From Thomas model	
							k_T (L/mg h)	q_T (mg/g)
2.42 (GHB)	2.85	0.014	0.176	0.986	17.54	20.45	0.080 ± 0.009	0.201 ± 0.009
8.35 (GHB)	2.85	0.013	0.169	0.633	32.12	5.92	0.296 ± 0.011	0.137 ± 0.006
8.35 (RGHB)	2.85	0.019	0.207	0.717	27.69	5.92	0.215 ± 0.014	0.174 ± 0.014
8.35 (GHB)	6.34	0.015	0.190	0.407	43.99	5.92	0.151 ± 0.007	0.203 ± 0.015

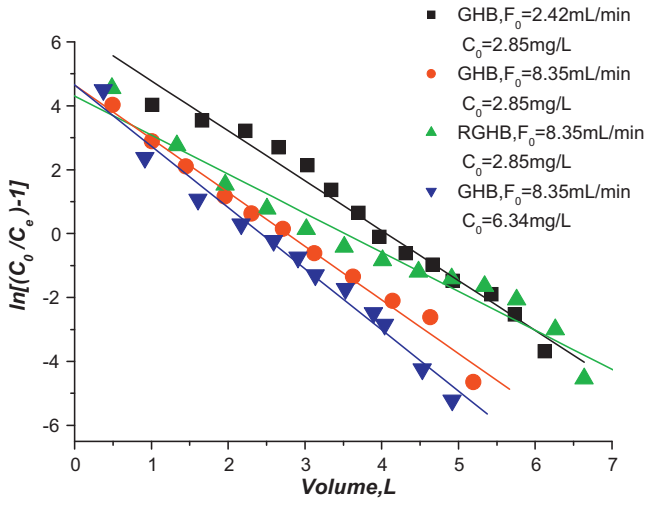

Fig. 7. Testing of experimental results by the Thomas equation for GHB and RGHB at different flow rate (F_0) and different initial fluoride concentration (C_0) (data from Fig. 6).

The linearized form of the Thomas model is as follows:

$$\ln\left[\left(\frac{C_0}{C_e}\right)-1\right]=\left(\frac{k_T q_T m}{\theta}\right)-\left(\frac{k_T C_0 V}{\theta}\right) \quad (16)$$

From experimental data for C_e, C_0, and t at different flow rates, graphical dependences were plotted in Fig. 7. The rate constant (k_T) and the total sorption capacity (q_T) can be determined by from a plot of $\ln[(C_0/C_e)-1]$ against t at a given flow rate. The model parameters were given in Table 5.

In order to provide an adequate test of the Thomas model equation, the total sorption capacity q_T calculated from Eq. (16) and q_E calculated from the area above the S curves up to the saturation point should be close to each other. The agreement of q_T and q_E (Table 5) confirmed the applicability of the Thomas model to the examined column system.

3.2.1. Effect of flow rate

Initially, most of the fluoride ions were adsorbed, hence the solute concentration in the effluent was low. As adsorption continued, the effluent concentration rose, slowly at first but then abruptly. At a lower flow rate of 2.42 mL/min, the adsorption with time was very efficient in the initial step of process. This fact was probably associated with the availability of reaction sites able to capture fluoride ions around or inside the cells. In the second stage, the uptake became less effective with the gradual occupancy of these sites. Even after breakthrough occurred, the column was still capable of accumulating fluoride although at a progressively lower efficiency.

With the increase of flow rate, the empty bed contact time (EBCT) decreased, while the height of the mass transfer zone (h_Z) increased; the breakthrough curve became steeper, breakthrough time decreased because of faster saturation of the fixed bed (Fig. 6). The residence time of the solute in the column was not long enough for adsorption equilibrium to be reached at that flow rate, the fluoride solution left the column before equilibrium occurred. Thus, at higher flow rate, the contact time of fluoride ions with GHB was very short, causing a reduction in removal efficiency.

The rate constant, k_T, increased with the increase of the flow rate which indicated that the mass transport resistance decreased. The mass transport resistance was proportional to axial dispersion and thickness of the liquid film on the particle surface [43]. The increase of the flow rate increased the driving force of mass transfer in the liquid film [26].

3.2.2. Effect of initial fluoride concentration

Initial fluoride concentration of 2.85 and 6.34 mg/L were used to study the column studies. Fluoride adsorbed by GHB in the packed column depended on the volume of flow passed. The effluent volume showed whether fluoride uptake by GHB was subjected to saturation limits. With the increase of initial fluoride concentration, the breakthrough curve became steeper, breakthrough time decreased because of faster saturation of the fixed bed (Fig. 6). As solution continued to flow, the concentration of fluoride in the effluent rapidly increased. Finally the bed became saturated with fluoride and the concentration of solute in the effluent rose to the inlet fluoride concentration.

The rate constant (k_T) and the breakthrough time decreased with the increase of the initial fluoride concentration. The breakthrough capacities (q_B) and exhaustion capacities (q_E) increased with the increase of initial fluoride concentration.

3.2.3. Column regeneration

At higher pH conditions, GHB has little sorption of fluoride (Fig. 3). Therefore, alkali can be used as a regenerant to adjust the pH in the solution to realize the fluoride desorption and regeneration of exhausted GHB. Fluoride removal of GHB and RGHB at flow rate of 8.35 mL/min and initial fluoride concentration of 6.34 mg/L were shown in Fig. 6. The total sorption capacity of GHB increased after regeneration and reactivation by using alkali/alum treatment. This was mainly because of the ion-exchange characteristics of bentonite. The Na^+ or H^+ on the bentonite was exchanged for Al^{3+} in the solution and the GHB had higher sorption capacity.

Additionally, the results showed that the sorption capacities of the columns were higher than their respective batch capacities (q_e = 0.094 mg/g for 12 g/L GHB dosage) for the same initial fluoride concentration (2.85 mg/L). Similar results were observed by Genç-Fuhrman et al. [46], Gupta et al. [47] and Tor et al. [26]. The reason for the observed discrepancies between the batch and column systems may be that GHB had pores that enhanced solid state diffusion relative to the batch tests [48]. Higher fluoride sorption capacity was obtained in column experiments than in batch experiments.

4. Conclusion

In this study, GHB was prepared and its fluoride sorption capacity was evaluated by batch and column adsorption experiments. The main conclusions from this study can be listed as follows:

(i) GHB can be used as a low-cost granular adsorbent in fluoride removal.

(ii) Batch experiments indicated that the time to attain equilibrium was 40 min and the adsorption followed the pseudo-second-order kinetic model.
(iii) The maximum adsorption or removal of fluoride was achieved at a pH of 4.95.
(iv) The adsorption of fluoride by GHB in batch systems can be described by the Freundlich isotherm, and the adsorption capacity (k) was 0.094 mg/g.
(v) The fluoride adsorption type of GHB was ion-exchange.
(vi) The breakthrough capacities (q_B) and exhaustion capacities (q_E) increased with the decrease of flow rate and the increase of initial fluoride concentration.
(vii) The height of the mass transfer zone (h_Z) increased and the empty bed contact time (EBCT) decreased with the increase of flow rate. The height of the mass transfer zone (h_Z) increased with the increase of initial fluoride concentration.
(viii) Exhausted GHB can be regenerated by alkali/alum treatment. The total sorption capacity of GHB increased after regeneration and activation. Regenerated GHB had higher breakthrough capacities (q_B) and exhaustion capacities (q_E).
(ix) The rate constant (k_T) increased and the breakthrough time decreased with the increase of the flow rate. The rate constant (k_T) decreased and the breakthrough time decreased with the increase of the of initial fluoride concentration.
(x) Higher fluoride sorption capacity was obtained in column experiments than in batch experiments.

Acknowledgements

The authors are grateful for the financial support by the National Natural Science Foundation of China (Grant No. 40872150), Heilongjiang Postdoctoral Foundation and Shandong Postdoctoral Foundation.

References

[1] V. Agrawal, A.K. Vaish, P. Vaish, Groundwater quality: focus on fluoride and fluorosis in Rajasthan, Curr. Sci. 73 (1997) 743–764.
[2] WHO (World Health Organization), Guidelines for Drinking Water Quality, World Health Organization, Geneva, 1993.
[3] Y. Cengeloglu, E. Kir, M. Ersoz, Removal of fluoride from aqueous solution by using red mud, Sep. Purif. Technol. 28 (2002) 81–86.
[4] A. Tor, Removal of fluoride from an aqueous solution by using montmorillonite, Desalination 201 (2006) 267–276.
[5] S. Meenakshi, N. Viswanathan, Identification of selective ion-exchange resin for fluoride sorption, J. Colloid Interface Sci. 308 (2007) 438–450.
[6] M.G. Sujana, R.S. Thakur, S.N. Das, S.B. Rao, Defluorination of waste waters, Asian J. Chem. 4 (1997) 561–570.
[7] F. Durmaz, H. Kara, Y. Cengeloglu, M. Ersoz, Fluoride removal by Donnan dialysis with anion exchange membranes, Desalination 177 (2005) 51–57.
[8] A. Tor, Removal of fluoride from water using anion-exchange membrane under Donnan dialysis condition, J. Hazard. Mater. 141 (2006) 814–818.
[9] E. Kir, E. Alkan, Fluoride removal by Donnan dialysis with plasma-modified and unmodified anion-exchange membranes, Desalination 197 (2006) 217–224.
[10] M. Hichour, F. Persin, J. Sandeaux, C. Gavach, Fluoride removal from waters by Donnan dialysis, Sep. Purif. Technol. 18 (2000) 1–11.
[11] N. Kabay, O. Arar, S. Samatya, U. Yuksel, M. Yuksel, Separation of fluoride from aqueous solution by electrodialysis: effect of process parameters and other ionic species, J. Hazard. Mater. 153 (2008) 107–113.
[12] S. Sourirajan, T. Matsurra, Studies on reverse osmosis for water pollution control, Water Res. 6 (1972) 1073–1086.
[13] R. Simons, Trace element removal from ash dam waters by nanofiltration and diffusion dialysis, Desalination 89 (1993) 325–341.
[14] L. Guo, B.J. Hunt, P.H. Santsci, Ultrafiltration behavior of major ions (Na, Ca, Mg, F, Cl, and SO_4) in natural waters, Water Res. 35 (6) (2001) 1500–1508.
[15] M. Srimurali, A. Pragathi, J. Karthikeyan, A study on removal of fluorides from drinking water by adsorption onto low-cost materials, Environ. Pollut. 99 (1998) 285–289.
[16] B. Kemer, D. Ozdes, A. Gundogdu, V.N. Bulut, C. Duran, M. Soylak, Removal of fluoride ions from aqueous solution by waste mud, J. Hazard. Mater. 168 (2009) 888–894.
[17] M. Yang, T. Hashimoto, N. Hoshi, H. Myoga, Fluoride removal in a fixed bed packed with granular calcite, Water Res. 33 (1999) 3395–3402.
[18] Y.H. Li, S. Wang, A. Cao, D. Zhao, X. Zhang, C. Xu, Z. Luan, D. Ruan, J. Liang, D. Wu, B. Wei, Adsorption of fluoride from water by amorphous alumina supported on carbon nanotubes, Chem. Phys. Lett. 350 (2001) 412–416.
[19] M. Mahramanlioglu, I. Kizilcikli, I.O. Bicer, Adsorption of fluoride from aqueous solution by acid treated spent bleaching earth, J. Flourine Chem. 115 (2002) 41–47.
[20] E. Oguz, Adsorption of fluoride on gas concrete materials, J. Hazard. Mater. 117 (2005) 227–233.
[21] G. Christidis, Physical and chemical properties of some bentonite deposits of Kimolos Island, Greece, Appl. Clay Sci. 13 (1998) 79–98.
[22] B. Bar-Yosef, I. Afik, R. Rosenberg, Fluoride sorption by montmorillonite and kaolinite, Soil Sci. 145 (1988) 194.
[23] P.M.H. Kau, D.W. Smith, P. Binning, Experimental analysis of fluoride diffusion and sorption in clays, Geoderma 84 (1998) 89–108.
[24] A. Kapoor, T. Viraraghavan, Use of immobilized bentonite in removal of heavy metals from wastewater, J. Environ. Eng. ASCE 124 (1998) 1020–1024.
[25] C. Zhu, Z. Luan, Y. Wang, X. Shan, Removal of cadmium from aqueous solutions by adsorption on granular red mud (GRM), Sep. Purif. Technol. 57 (2007) 161–169.
[26] A. Tor, N. Danaoglu, G. Arslan, Y. Cengeloglu, Removal of fluoride from water by using granular red mud: batch and column studies, J. Hazard. Mater. 164 (2009) 271–278.
[27] T.Z. Zhang, Y.C. Shi, H.L. Wang, B.H. Xu, Ecology of nonmetallic deposits in Shandong, Shandong Sci. Technol. Jinan (1998) 145–165 (in Chinese).
[28] L.D. Benefield, J.F. Judkins, B.L. Weand, Process Chemistry for Water and Wastewater Treatment, Prentice-Hall, Inc., New Jersey, 1982.
[29] S. Lagergren, K. Svenska, About the theory of so called adsorption of soluble substances, K. Sven. Vetenskapsad. Handl. 24 (1898) 1–39.
[30] Y.S. Ho, G. McKay, Pseudo-second order model for sorption processes, Process Biochem. 34 (1999) 451–465.
[31] G. McKay, The adsorption of basic dye onto silica from aqueous solution–solid diffusion model, Chem. Eng. Sci. 39 (1984) 129–138.
[32] G. Lagaly, S. Ziesmer, Colloid chemistry of clay minerals: the coagulation of montmorillonite dispersions, Adv. Colloid Interface Sci. 100–110 (2003) 105–128.
[33] G. Lagaly, Coagulation and Flocculation, Theory and Applications, M. Dekker, New York, 1993, pp. 427–1215.
[34] K. Tanabe, Solid Acids and Bases, Academic Press, New York, 1970.
[35] J. Ravichandran, B. Sivasankar, Properties and catalytic activity of acid-modified montmorillonite and vermiculite, Clay. Clay Miner. 45 (1997) 854–858.
[36] T. Alemdaroğlu, G. Akkuş, M. Önal, Y. Sarikaya, Investigation of the surface acidity of a bentonite modified by acid activation and thermal treatment, Turk. J. Chem. 27 (2003) 675–681.
[37] I. Langmuir, The constitution and fundamental properties of solids and liquids, J. Am. Chem. Soc. 38 (1916) 2221–2295.
[38] H.M.F. Freundlich, Über die adsorption in losungen, Z. Phys. Chem. 57A (1906) 385–470.
[39] O. Redlich, D.L. Peterson, A useful adsorption isotherm, J. Phys. Chem. 63 (1959) 1024.
[40] H. Genç-Fuhrman, J.C. Tjell, D. McConchie, Adsorption of arsenic from water using activated neutralized red mud, Environ. Sci. Technol. 38 (2004) 2428–2434.
[41] R. Qadeer, J. Hanif, Adsorption of uranium in the presence of different cations on activated charcoal, J. Chem. Soc. Pak. 15 (1993) 227–230.
[42] R. Qadeer, J. Hanif, M. Khan, M. Salem, Uptake of uranium ions by molecular-sieve, Radiochim. Acta 68 (1995) 197–201.
[43] N. Vukojevic Medvidovic, J. Peric, M. Trgo, M.N. Muzek, Removal of lead ions by fixed bed of clinoptilolite—the effect of flowrate, Sep. Purif. Technol. 49 (2006) 298–304.
[44] Z. Aksu, F. Gonen, Biosorption of phenol by immobilized activated sludge in a continuous packed bed: prediction of breakthrough curves, Process Biochem. 39 (2004) 599–613.
[45] H.C. Thomas, Heterogeneous ion exchange in a flowing system, J. Am. Chem. Soc. 66 (1944) 1664–1666.
[46] H. Genç-Fuhrman, H. Bregnhøj, D. McConchie, Arsenate removal from water using sand-red mud columns, Water Res. 39 (2005) 2944–2954.
[47] V. Gupta, M. Gupta, S. Sharma, Process development for the removal of lead and chromium from aqueous solutions using red mud, an aluminium industry waste, Water Res. 35 (2001) 1125–1134.
[48] E. Lopez, B. Soto, M. Arias, A. Nunez, D. Rubinos, M.T. Barral, Adsorbent properties of red mud and its use for wastewater treatment, Water Res. 32 (1998) 1314–1322.